Published in The Journal of Biological Chemistry 78, issue 40, 38617-38627, 2003
which should be used for any reference to this work

atTic110 Functions as a Scaffold for Coordinating the Stromal Events of Protein Import into Chloroplasts*

Takehito Inaba‡§, Ming Li‡, Mayte Alvarez-Huerta¶, Felix Kessler¶, and Danny J. Schnell‡‖

‡ *Department of Biochemistry and Molecular Biology, University of Massachusetts, Amherst, Massachusetts 01003*
¶ *Laboratoire de Physiologie Végétale, Institut de Botanique, Université de Neuchâtel, Neuchâtel 2007, Switzerland*

The translocon of the inner envelope membrane of chloroplasts (Tic) mediates the late events in the translocation of nucleus-encoded preproteins into chloroplasts. Tic110 is a major integral membrane component of active Tic complexes and has been proposed to function as a docking site for translocation-associated stromal factors and as a component of the protein-conducting channel. To investigate the various proposed functions of Tic110, we have investigated the structure, topology, and activities of a 97.5-kDa fragment of *Arabidopsis* Tic110 (atTic110) lacking only the amino-terminal transmembrane segments. The protein was expressed both in *Escherichia coli* and *Arabidopsis* as a stable, soluble protein with a high α-helical content. Binding studies demonstrate that a region of the atTic110-soluble domain selectively associates with chloroplast preproteins at the late stages of membrane translocation. These data support the hypothesis that the bulk of Tic110 extends into the chloroplast stroma and suggest that the domain forms a docking site for preproteins as they emerge from the Tic translocon.

Chloroplast biogenesis is dependent upon the import of ~3000 different nucleus-encoded proteins (1). The majority of these proteins are synthesized as preproteins carrying an amino-terminal transit peptide that serves as the essential signal for targeting to the organelle. The transit peptide is recognized by receptor components of the translocon at the outer envelope membrane of chloroplasts (Toc), and a GTP-regulated switch initiates translocation through the protein-conducting channel of the Toc complex. At this stage, the Toc complex associates with the translocon at the inner envelope membrane (Tic), and this Toc-Tic supercomplex mediates the direct transport of the preproteins from the cytoplasm into the chloroplast stroma (2).

Although many mechanistic details remain to be defined, the activities of the Toc components have been extensively investigated. Two membrane-associated GTPases, Toc159 and Toc34/33, mediate transit peptide recognition and regulate the initiation of translocation (3–7). The Toc GTPases form a complex with Toc75, an integral membrane protein that, along with Toc159, constitutes a major component of the protein-conducting channel (1, 8–10).

* This work was supported by National Science Foundation Grant MCB-0090727 (to D. J. S.). The costs of publication of this article were defrayed in part by the payment of page charges. This article must therefore be hereby marked "*advertisement*" in accordance with 18 U.S.C. Section 1734 solely to indicate this fact.

§ Recipient of a Japan Society for the Promotion of Science postdoctoral fellowship for research abroad.

‖ To whom correspondence should be addressed. Tel.: 413-545-4024; Fax: 413-545-3291; E-mail: dschnell@biochem.umass.edu.

In contrast to the Toc complex, the activities and functions of the Tic components are less well defined. The biochemical analysis of Tic function has been complicated by the fact that assembly of functional Tic complexes is dynamic and occurs in response to preprotein translocation (11). Therefore, the isolation of a stable Tic complex has thus far been elusive. Tic110 was the first Tic component identified and represents a major component of active Tic complexes (12, 13). It is an integral inner envelope membrane protein, and structural predictions suggest that it consists of two predicted transmembrane helices at its extreme amino terminus and a 97.5-kDa carboxyl-terminal region that is largely hydrophilic. Tic110 transiently associates with at least five other Tic proteins. These include Tic20, a polytopic membrane protein that is implicated in protein translocation at the inner membrane by covalent cross-linking and genetic studies (11, 14); Tic22, a peripheral inner membrane protein that may regulate interactions between the Toc and Tic translocons by sensing preprotein emergence into the intermembrane space (11, 15); Tic40, an inner membrane protein that appears to interact with preproteins at late stage in inner membrane translocation (16); and Tic55 and Tic62, two inner membrane redox components that are proposed to serve as regulators of the translocation reaction (17, 18).

Studies of Tic110 topology and molecular interactions have led to three models for its roles in protein import. In the first model, the carboxyl-terminal region of pea Tic110, psTic110, was predicted to extend into the intermembrane space between the outer and inner envelope membranes and thereby mediate the interactions between the Toc and Tic complexes during the translocation reaction (13, 19). However, this model was discounted by detailed topology mapping studies (20). The results indicated that psTic110 exists in the opposite orientation with the bulk of the protein extending into the stroma and limited exposure to the intermembrane space. In the second model, the large hydrophilic domain of Tic110 is proposed to serve as a docking site for soluble stromal chaperones that assist in the translocation and folding of imported proteins (12, 20). In this scenario, Tic110 would function in a manner analogous to Tim44, a protein that mediates mtHsp70 localization to the matrix face of the Tim23 translocon in mitochondria (21). This model is supported by the topology studies and by the observation that native psTic110 associates reversibly with the Hsp93 and Cpn60 chaperones of the chloroplast stroma (12, 22). Recently, this model has been challenged by a third hypothesis. This study proposed that Tic110 is a β-barrel membrane protein and functions as the protein-conducting channel of the Tic translocon (23). These conclusions were based on the observation that a urea-denatured fragment of psTic110 gave rise to ion channels when inserted into proteoliposomes. However, the relevance of the reconstitution data are unclear because native psTic110 does not form similar channels in recon-

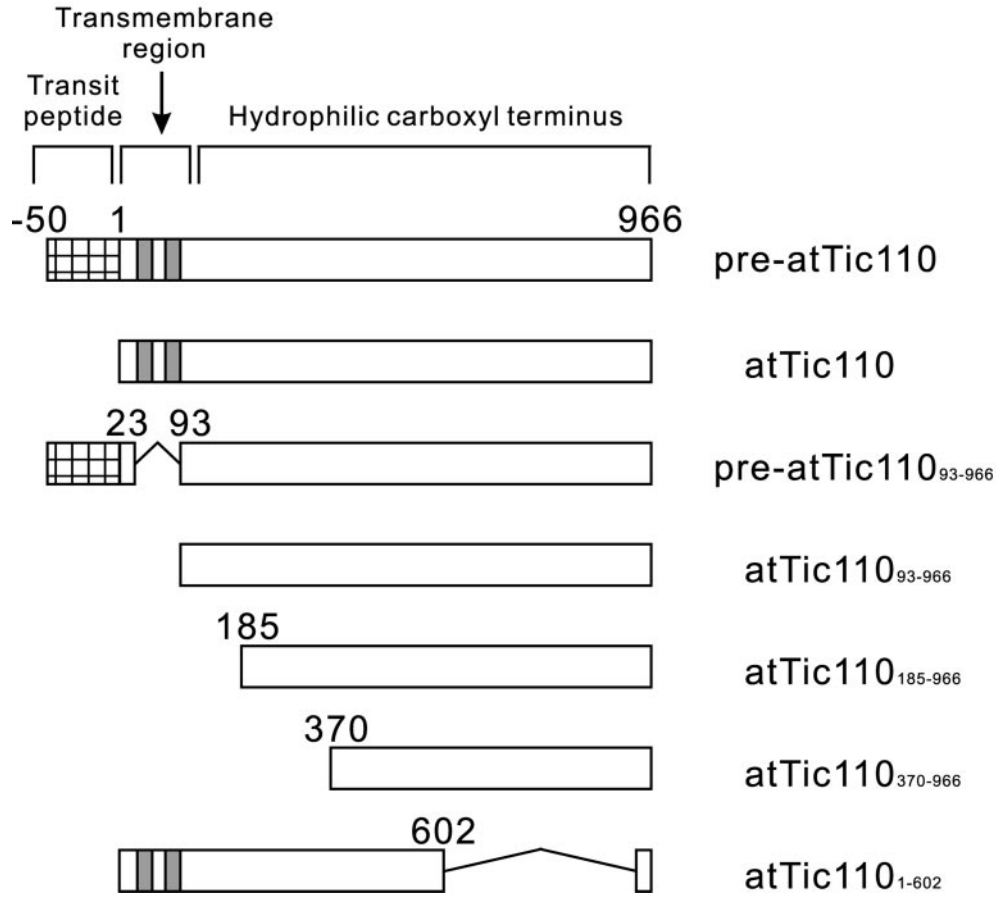

FIG. 1. **Schematic diagram of the constructs used in this study.** The predicted transmembrane domains are shown with *shaded boxes*. The *hatched boxes* indicate the transit peptide. The *numbers* refer to the amino acid positions, with +1 indicating the amino-terminal residue of mature atTic110.

stituted proteoliposomes, nor are similar channels observed in native chloroplast envelope membranes (23).

To examine these three models, we have investigated the structure, topology, and function of *Arabidopsis* Tic110, atTic110. We demonstrate that the 97.5-kDa carboxyl-terminal region of atTic110 lacking only the two predicted transmembrane domains (atTic110$_{93–996}$) exists as a soluble protein when expressed in *Escherichia coli* and when targeted to chloroplasts *in vivo*. Circular dichroism spectra indicate that this region is predominantly α-helical, consistent with secondary structure predictions. Furthermore, we demonstrate that native Tic110 purified from pea chloroplasts and recombinant atTic110$_{93–996}$ bind selectively to chloroplast preproteins. The transit peptide-binding domain maps to a site on atTic110$_{93–996}$ that is predicted to localize close to the stromal face of the Tic translocon. These data support the hypothesis that Tic110 acts as a scaffold to coordinate the stromal events of protein translocation into chloroplasts and are inconsistent with a role for Tic110 as a β-barrel channel.

EXPERIMENTAL PROCEDURES

Construction of atTic110 Deletion Mutants and Arabidopsis Transformation—The pre-atTic110 cDNA was amplified from total *Arabidopsis* cDNA by reverse transcription-PCR using primers that introduced 5′ *Xho*I and *Bsp*HI sites spanning the start codon and a 3′ *Xba*I site following the stop codon. The cDNA was inserted into the *Xho*I and *Xba*I sites of pBluescript SK+ to generate pBS-pre-atTic110 and the *Nco*I and *Xba*I sites of pCAMBIA3300.1 to generate pCAMBIA-pre-atTic110. The mature atTic110 construct and the deletion construct atTic110$_{93–966}$ were generated using PCR with primers that introduced *Xho*I and *Bsp*HI sites containing start codons immediately upstream from the amino-terminal codons of the constructs and *Xba*I sites following the stop codons of the open reading frames. A full-length atTic110 cDNA clone (pBS-pre-atTic110) or an identical clone encoding the addition of a carboxyl-terminal hexahistidine tag (pBS-atTic110-His) was used as the template. The PCR products were introduced into the *Xho*I and *Xba*I sites of pBlueScript SK+ to generate pBS-atTic110 and pBS-atTic110$_{93–966}$. The pBluescript clones were digested with *Bsp*HI and *Not*I and subcloned into the *Nco*I and *Not*I sites of pET21d to generate pET21d-atTic110 and pET21d-atTic110$_{93–966}$. The fragments of atTic110$_{185–966}$ and atTic110$_{370–966}$ were generated by PCR with primers that introduced *Xho*I sites and *Bsp*HI sites containing start codons immediately upstream from the amino-terminal codons of the constructs and *Not*I site following the stop codons of the open reading frames. The PCR products were directly digested with *Bsp*HI and *Not*I and subcloned into the *Nco*I and *Not*I sites of pET21d to generate pET21d-atTic110$_{185–966}$ and pET21d-atTic110$_{370–966}$. The pBS-atTic110$_{1–602}$ construct encoding atTic110$_{1–602}$ was generated by digestion of pBS-atTic110 with *Eco*RV and *Pst*I, treatment with *Pfu* DNA polymerase to generate blunt ends, and self-ligation. The pBS-atTic110$_{1–602}$ was then digested with *Bsp*HI and *Not*I and subcloned into the *Nco*I and *Not*I sites of pET21d to generate pET21d-atTic110$_{1–602}$. The pCAMBIA-pre-atTic110$_{93–966}$ construct encoding pre-atTic110$_{93–966}$ was generated by digesting pCAMBIA-pre-atTic110 with *Nco*I and *Xba*I and replacing the atTic110 3′ fragment with the *Bsp*HI-*Xba*I fragment of pBS-atTic110$_{93–966}$. All of the constructs were confirmed by DNA sequencing.

The pCAMBIA-pre-atTic110$_{93–966}$ and pCAMBIA-pre-atTic110 constructs were introduced into *Arabidopsis thaliana* (ecotype Wassilewskija) via *Agrobacterium tumefaciens*-mediated transformation by the floral dip method (14). Transformed plants were selected on BASTA, and the presence of the transgene was confirmed by PCR of genomic DNA using transgene-specific primers (data not shown).

In Vitro Translation and Expression in E. coli—All of the ^{35}S-labeled *in vitro* translation products were generated in a coupled transcription-translation system containing reticulocyte lysate according to the manufacturer's recommendations (Promega) using the pET21d constructs encoding the atTic110 constructs.

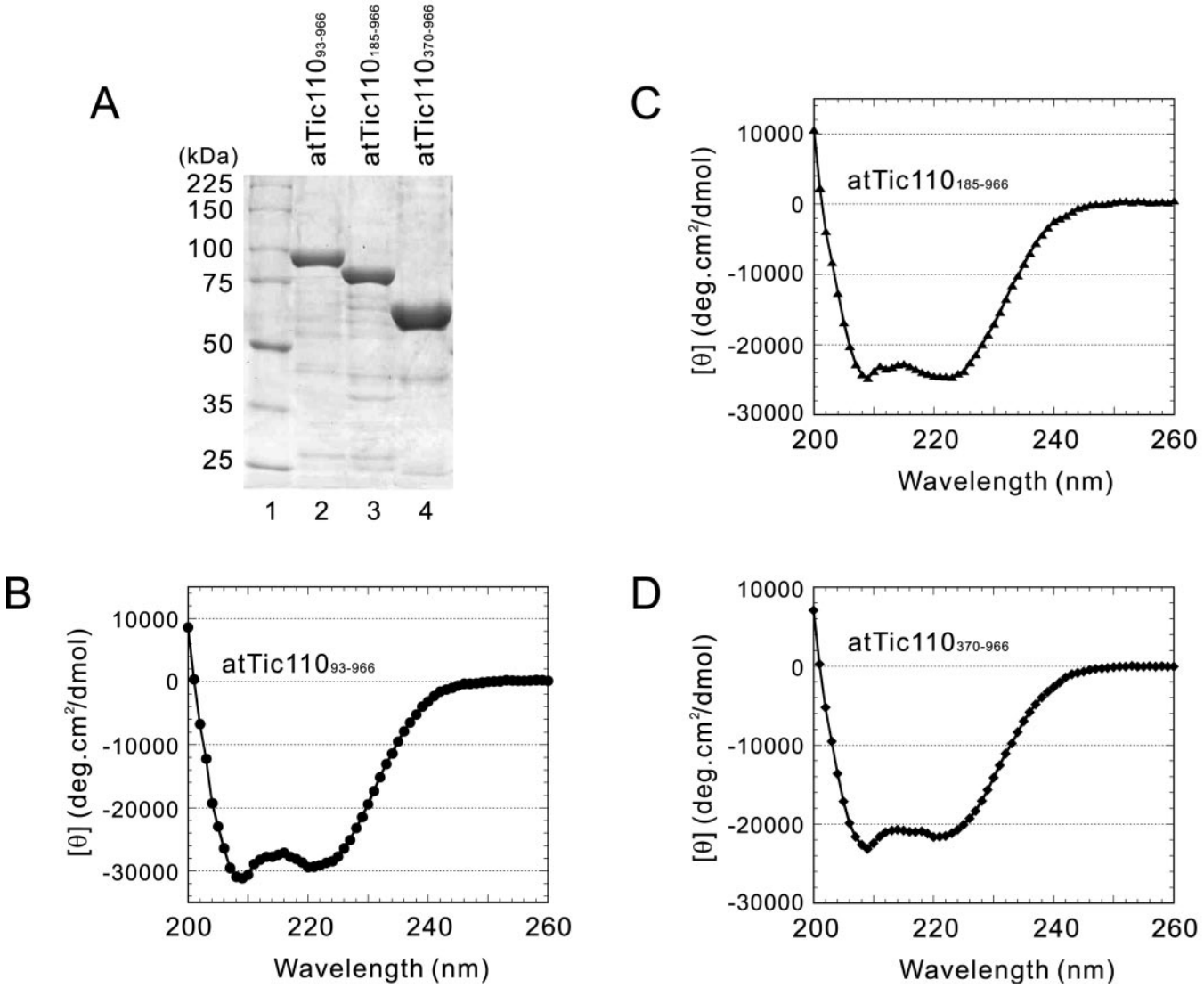

FIG. 2. **Expression of atTic110 deletion mutants in *E. coli* and their circular dichroism spectra.** *A*, SDS-PAGE profile of the indicated recombinant atTic110 deletion mutants purified from soluble *E. coli* extracts by nickel-NTA chromatography. The molecular sizes of standard proteins (*lane 1*) are indicated to the *left* of the figure. The polypeptides were visualized by staining with Coomassie blue. *B–D*, circular dichroism spectra of atTic110$_{93–966}$ (*B*), atTic110$_{185–966}$ (*C*), and atTic110$_{370–966}$ (*D*). Note that the negative bands at 208 and 222 nm are typically observed in proteins with substantial α-helical structure.

For bacterial expression, pET21d-atTic110$_{93–966}$-His, pET21d-atTic110$_{185–966}$-His, and pET21d-atTic110$_{370–966}$-His were transformed into *E. coli* BL21(DE3). Expression was induced with 0.2 mM isopropyl-1-thio-β-D-galactopyranoside overnight at 20 °C. The proteins were purified from soluble *E. coli* extracts of under nondenaturing conditions using nickel-NTA[1] resin (Novagen, Inc.). The proteins were stored in 40 mM Tris-HCl, pH 8.0, 1 M NaCl, 250 mM imidazole, and 0.02% NaN_3 at +4 °C or −80 °C.

Structural Analysis—CD spectra of proteins were measured in 50 mM sodium phosphate buffer, pH 8.0, at a concentration of 5 μM proteins on an AVIV 62DS CD spectrophotometer (Aviv Associates, Inc., Lakewood, NJ). The α-helical content was estimated from the mean residue ellipticity at 222 nm according to Ref. 24. The secondary structure was also predicted by the PSIPRED secondary structure prediction method (25).

Arabidopsis Chloroplast Isolation and Immunoblotting—Wild type and transgenic *Arabidopsis* were grown on soil under 18-h day conditions. Chloroplasts were isolated from 3-week-old seedlings as described previously (26) with the omission of bovine serum albumin from all buffers. Isolated intact chloroplasts were separated into membrane and soluble fractions by lysis in 0.1 M Na_2CO_3, pH 11.5, followed by centrifugation at 200,000 × *g* for 20 min. The pellets (membrane fraction) were directly dissolved in 350 mM Tris base, pH 11.0, 5% sodium dodecyl sulfate, 10% glycerol, and 80 mM dithiothreitol (SDS-PAGE sample buffer). The soluble proteins were recovered by precipitation with trichloroacetic acid and dissolved into SDS-PAGE sample buffer. Intact chloroplasts were treated with 20 μg/ml trypsin as described previously (11). The reisolated chloroplasts were analyzed by SDS-PAGE and immunoblotting.

Total protein extracts from *Arabidopsis* were obtained by directly homogenizing leaves in SDS-PAGE sample buffer. For fractionation of total membrane and soluble proteins, *Arabidopsis* leaves were homogenized in 50 mM Hepes-KOH, pH 7.5, 0.45 M sucrose, 2 mM dithiothreitol, and 2 mM EDTA. The homogenate was filtered through two layers of Miracloth and centrifuged at 500 × *g* for 2 min. The supernatant was diluted to either 2 mM ice-cold EDTA or 0.1 M Na_2CO_3, pH 11.5, and separated into membrane and soluble fractions as described above and analyzed by SDS-PAGE and immunoblotting. All of the samples were resolved by SDS-PAGE, transferred to nitrocellulose membrane, and immunoblotted with anti-atTic110, anti-atToc33, and anti-atToc75 serums as described previously (14).

Pea Chloroplast Isolation and Preprotein Cross-linking—Intact chlo-

[1] The abbreviations used are: NTA, nitrilotriacetic acid agarose; Tricine, *N*-[2-hydroxy-1,1-bis(hydroxymethyl)ethyl]glycine; DHFR, dihydrofolate reductase; PIRAC, protein import related anion channel; CRABP, cellular retinoic acid-binding protein; rubisco, ribulose-bisphosphate carboxylase/oxygenase; APDP, *N*-[4-(*p*-azidosalicylamido)butyl]-3′(2-pyridyldithio)propionamide; SSU, small subunit of rubisco.

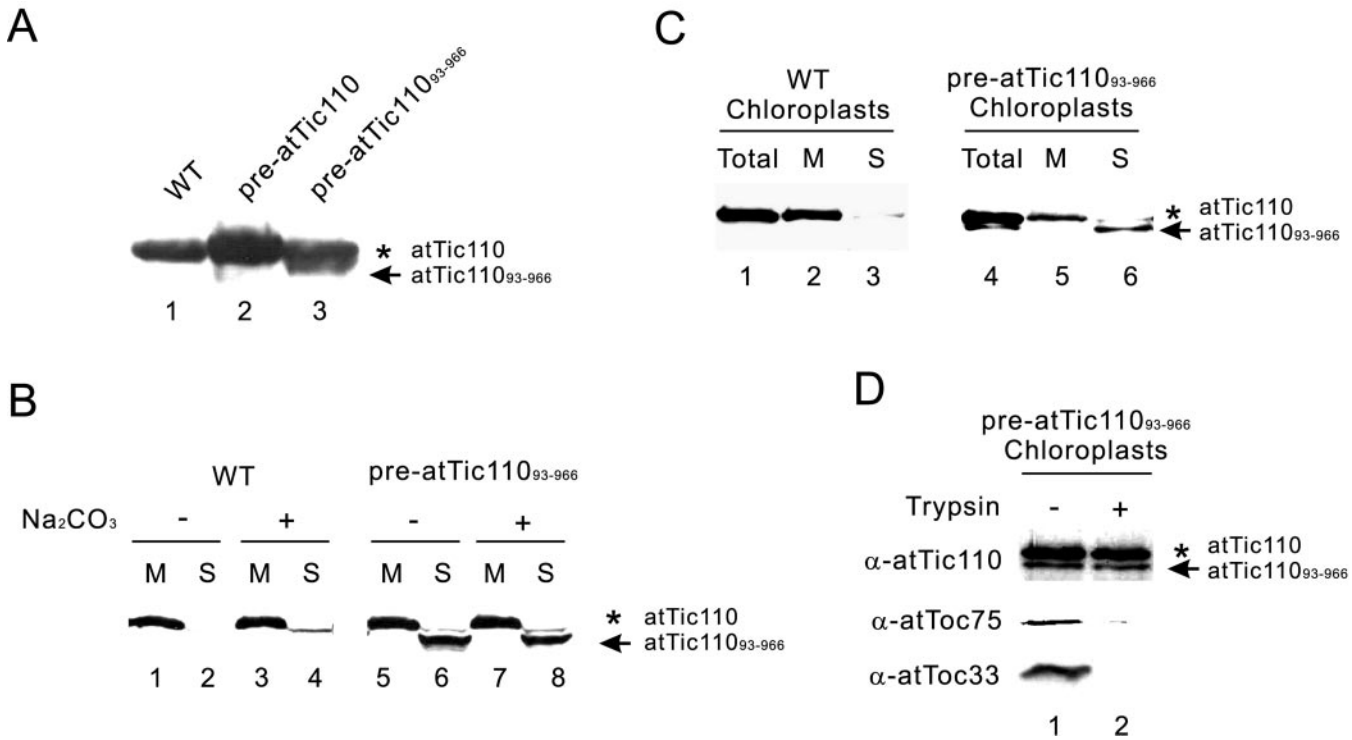

FIG. 3. **Localization of atTic110 and atTic110$_{93–966}$ proteins in transgenic *Arabidopsis*.** *A*, immunoblots of total protein extracts from wild type (*WT*) plants (*lane 1*) and transgenic plants expressing pre-atTic110 (*lane 2*) or pre-atTic110$_{93–966}$ (*lane 3*) with antibodies raised against atTic110. Each lane contains 100 μg of total protein extract. *B*, localization of atTic110 and atTic110$_{93–966}$ in soluble and membrane fractions of total extracts from wild type and transgenic plants. Total protein extracts from wild type or atTic110$_{93–966}$ transgenic plants were separated into membrane (*M*) or soluble (*S*) fractions in the presence or absence of sodium carbonate. The membrane (30 μg of total protein) and soluble (100 μg of total protein) extracts were resolved by SDS-PAGE and immunoblotted with anti-atTic110. *C*, localization of atTic110 and atTic110$_{93–966}$ in chloroplasts. Isolated intact chloroplasts (*Total*, 50 μg of total protein) from wild type or atTic110$_{93–966}$ transgenic plants or their corresponding membrane (*M*) and soluble (*S*) fractions were resolved by SDS-PAGE and immunoblotted with anti-atTic110 serum. *D*, trypsin sensitivity of atTic110 and atTic110$_{93–966}$ in intact chloroplasts. Chloroplasts equivalent to 25 μg of chlorophyll were treated with 20 μg/ml of trypsin on ice for 30 min. Intact chloroplasts were reisolated, resolved by SDS-PAGE, and probed with anti-atTic110, anti-atToc75, and anti-atToc33. The positions of atTic110 and the atTic110$_{93–966}$ deletion mutant are indicated to the *right* of each figure.

roplasts were isolated from 10–14-day-old pea seedlings (*Pisum sativum* var. Green Arrow) as previously described (11). The modification of pFd-protA with [^{125}I]APDP and covalent cross-linking reactions with intact chloroplasts were performed as previously described (9, 27). The cross-linked products were analyzed on 7.5–15% SDS-PAGE gradient gels to resolve proteins in the 60–150-kDa range. Thermolysin treatment of intact chloroplasts was performed as described previously (8) using 0.2 mg protease/ml for 30 min on ice.

To prepare chloroplast envelope membranes, intact chloroplasts were lysed under hypertonic conditions and separated into soluble and membrane fractions by differential centrifugation as described by Keegstra and Yousif (28). The total membrane fraction was separated into envelope and thylakoid membrane fractions by flotation into linear sucrose gradients as previously described (8). The envelope fractions were analyzed by SDS-PAGE. The radioactive signals in dried gels were captured and quantitated using a PhosphorImager SI (Molecular Dynamics, Sunnyvale, CA) with the IPLab Gel Scientific Image Processing version 1.5c program (Signal Analytics, Vienna, VA).

Immunoaffinity Chromatography and Immunoprecipitation Reactions—Envelope membranes corresponding to a mixed outer/inner membrane population were used for all immunoaffinity chromatography reactions. The envelope membranes were purified by the method described previously (11). For immunoaffinity chromatography under native conditions, the membranes (100 μg of protein) were solubilized in 50 mM Tricine-KOH, 2 mM EDTA, and 150 mM NaCl (TES buffer) with 1% (w/v) Triton X-100 for 10 min on ice. The extract was clarified by centrifugation at 100,000 $\times$ *g* for 30 min to remove insoluble aggregates. The supernatant was diluted in half and incubated in the presence of 2 mM $MgCl_2$ and 1 mM ATP at 26 °C for 5 min. The sample was applied sequentially to IgG-Sepharose of anti-psToc34 IgG-Sepharose, anti-psToc86 IgG-Sepharose, and anti-psToc110 IgG-Sepharose (1 ml of packed matrix containing 5 mg of bound IgG). The Sepharose was washed with 10 volumes of TES buffer containing 0.2% (w/v) Triton X-100 and eluted with 0.2 M glycine, pH 2.2, containing 0.2% (w/v) decyl maltoside. The elutes and unbound fractions were analyzed by SDS-PAGE and immunoblotting.

The binding of [^{35}S]pre-SSU and [^{35}S]SSU to immunoadsorbed psTic110 was performed with anti-psTic110 IgG-Sepharose (0.5 ml of packed matrix containing 2.5 mg of bound IgG) containing bound psTic110 from envelope membranes (50 μg of protein) that had been subjected to the sequential immunoprecipitation as given above. The [^{35}S]pre-SSU and [^{35}S]SSU translation products were diluted 40-fold with 50 mM Hepes-KOH, pH 7.5, 50 mM KOAc, 4 mM $MgCl_2$, 0.1% Triton X-100 (wash buffer) and incubated with the anti-psTic110 IgG-Sepharose containing bound psTic110 for 30 min at 4 °C. The resin was washed five times with an excess of wash buffer, and bound protein was eluted with 0.2 M glycine, pH 2.2, 0.1% Triton X-100. The elutes were analyzed by SDS-PAGE and phosphorimaging.

Immunoprecipitation of psTic110 from chloroplast envelope membranes under denaturing conditions following covalent cross-linking was performed by the method of Anderson and Blobel (29). Before immunoprecipitation, the envelope membranes (100 μg of protein) were reduced with β-mercaptoethanol to cleave the cross-linker as described previously (9).

atTic110 Binding Assays—pFd-protA, Fd-protA, pSSU-DHFR, and DHFR were expressed in *E. coli* and purified on nickel-NTA resin as described previously (27). Purified pFd-protA and Fd-protA (30 pmol each), or pSSU-DHFR and DHFR (250 pmol each) were diluted in 20 mM Hepes-KOH, pH 7.5, 200 mM NaCl, and 0.1% Triton X-100 (binding buffer) to give a final concentration of 40 mM imidazole. The samples were bound to 8 μl of packed nickel-NTA resin at room temperature for 30 min under constant mixing. The resin was washed once with 400 μl of binding buffer containing 40 mM imidazole. The resin was incubated with *in vitro* translated [^{35}S]atTic110 or the [^{35}S]atTic110 deletion mutants in binding buffer containing 40 mM imidazole for 1 h at room temperature under constant mixing. The resin was washed three times with 400 μl of ice-cold binding buffer containing 40 mM imidazole. The bound proteins were eluted from the resin with SDS-PAGE sample

buffer containing 1 M imidazole and resolved by SDS-PAGE.

For the competition assays, purified pFd-protA (30pmol) was diluted in 20 mM Tris-HCl, pH 7.5, 150 mM NaCl (TBS buffer), and the samples were bound to 8 μl of packed IgG-Sepharose at room temperature for 1 h. The IgG-Sepharose was washed once with 400 μl of TBS buffer. The IgG-Sepharose was incubated with purified competitor (atTic110$_{93-966}$, atTic110$_{185-966}$, atTic110$_{370-966}$, or CRABP) for 30 min at room temperature under constant mixing. After preincubation with competitor, *in vitro* translated [^{35}S]atTic110 or [^{35}S]atTic110$_{1-602}$ was added and incubated for 1 h at room temperature under constant mixing. The resin was washed three times with 400 μl of ice-cold TBS buffer. The proteins were eluted from IgG-Sepharose with incubation in 0.2 M glycine, pH 2.2, for 15 min at room temperature under constant mixing. The eluates were resolved directly by SDS-PAGE.

All of the samples were analyzed on a Storm 840 PhosphorImager using ImageQuant 1.2 software (Molecular Dynamics). The quantitative binding data are presented as percentages of maximal binding observed with each translation product.

RESULTS

Structural and Topological Analyses of Recombinant atTic110—As a first step in our analysis of atTic110 function, we examined the structural features of the native protein. The primary structure of atTic110 contains two distinguishing features, a short amino-terminal region (residues 1–93) containing two α-helical transmembrane segments and a 97.5-kDa carboxyl terminus that is largely hydrophilic in nature (Fig. 1). We generated a series of truncated atTic110 constructs lacking only the two transmembrane domains (atTic110$_{93-966}$) or the transmembrane domains and additional portions of the amino terminus (atTic110$_{185-966}$ and atTic110$_{370-966}$) (Fig. 1). All of the constructs were successfully expressed and purified as soluble proteins in *E. coli* (Fig. 2*A*) with only a minor fraction of each (~10–15%) found in insoluble inclusion bodies (data not shown). The yields ranged from 5 to 10 mg/liter of *E. coli* culture. The purified fractions were stable to freeze-thaw cycles at concentration up to 5 mg/ml. These data indicate that the proteins are expressed in their native conformations and establish that the 97.5-kDa carboxyl-terminal region folds into a stable, soluble domain.

A variety of secondary structure predictions of both atTic110 and psTic110 suggest that the carboxyl-terminal region contains predominantly α-helical content. We examined the secondary structure of recombinant atTic110$_{93-966}$ by CD spectroscopy. The recombinant protein exhibited two strong negative bands at 208 and 222 nm that are typically observed in proteins with substantial α-helical content (Fig. 2*B*). The protein is predicted to contain at least 60–80% α-helices based on the θ_{222} value of −29,088 (24). The CD spectra of atTic110$_{185-966}$ and atTic110$_{370-966}$ give slightly less negative θ_{222} values, yet both are predicted to contain at least 50% α-helical content (Fig. 2, *C* and *D*). These results indicate that the bulk of native atTic110 consists of α-helical structure.

To further examine whether atTic110$_{93-966}$ was soluble or membrane-integrated, we generated transgenic *Arabidopsis* expressing either pre-atTic110, the authentic precursor to atTic110, or pre-atTic110$_{93-966}$, a construct corresponding to atTic110$_{93-966}$ fused to the atTic110 transit peptide (Fig. 1). The expression of both proteins was confirmed by immunoblotting of total tissue extracts using anti-atTic110 antibodies. The results from representative transformants for each construct are shown in Fig. 3*A*. As predicted, the pre-atTic110 transformant expressed elevated levels of atTic110 compared with wild type (Fig. 3*A*, compare *lanes 1* and *2*), whereas the pre-atTic110$_{93-966}$ transformant contained an additional 99.6-kDa band not observed in wild type plants (Fig. 3*A*, *lane 3*, *arrow*). The 99.6-kDa polypeptide corresponds to the hexahistidine-tagged atTic110$_{93-966}$ after processing to remove the transit peptide by the stromal processing peptidase.

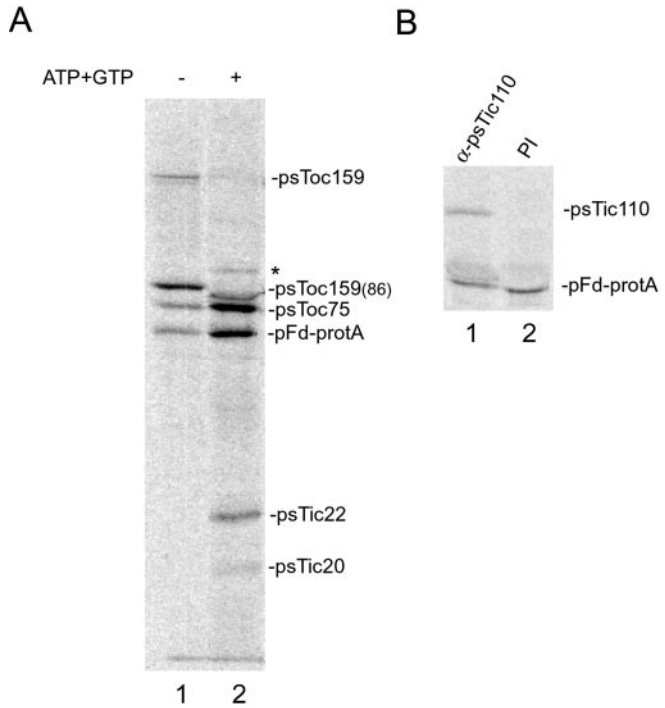

FIG. 4. **Cross-linking of envelope-bound pFd-protA-[^{125}I]APDP to psTic110.** *A*, energy-depleted pea chloroplasts were incubated with 200 nM urea denatured pFd-protA-[^{125}I]APDP in a standard import assay in the absence (−) or presence (+) of 0.1 mM ATP and GTP, and cross-linking was induced by photoactivation with UV irradiation. The total chloroplast envelope fraction was isolated and subjected to SDS-PAGE and phosphorimaging analysis. The positions of known Toc and Tic components are indicted at the *right* of the figure. The *asterisk* indicates the position of a 110-kDa cross-linked polypeptide. *B*, the envelope membrane fraction from pFd-protA-[^{125}I]APDP cross-linked chloroplasts (*lane 2*, *A*) was dissolved under denaturing conditions and immunoprecipitated with anti-psTic110 (*lane 1*) or preimmune serum (*PI*, *lane 2*). The positions of psTic110 and pFd-protA are shown to the *right* of the figure.

Separation of the soluble and membrane fractions by lysis in buffer at neutral or alkaline pH demonstrated that authentic atTic110 was exclusively membrane-associated (Fig. 3*B*, compare *lanes 1* and *2* and *lanes 3* and *4*). In contrast, atTic110$_{93-966}$ was observed exclusively in the soluble fraction under either lysis condition (Fig. 3*B*, *lanes 6* and *8*, *arrow*). To confirm that pre-atTic110$_{93-966}$ was targeted to chloroplasts, we isolated chloroplasts from wild type and atTic110$_{93-966}$ transgenic plants. The relative proportion of authentic atTic110 and atTic110$_{93-966}$ was similar to those observed in the total plant extracts (Fig. 3, *A* and *C*), indicating that pre-atTic110$_{93-966}$ was imported into chloroplasts. Separation of chloroplasts into soluble and membrane fractions indicated that atTic110 was almost exclusively found in the membrane fraction (Fig. 3*C*, compare *lanes 2* and *3*). However, atTic110$_{93-966}$ appeared only in the soluble fraction (Fig. 3*C*, compare *lanes 5* and *6*), indicating that the protein localized to the chloroplast stroma. The stromal localization of atTic110$_{93-966}$ was further confirmed by trypsin treatment of isolated intact chloroplasts. Trypsin is capable of permeating the outer membrane but not the inner membrane of intact chloroplasts (11, 12, 20). Both authentic atTic110 and atTic110$_{93-966}$ were resistant to trypsin treatment, whereas the outer membrane components, atToc75 and atToc33, were digested (Fig. 3*D*, compare *lanes 1* and *2*), indicating that atTic110$_{93-966}$ localized in the stroma. These data confirm that atTic110$_{93-966}$ folds into a soluble domain and support the conclusion that the predicted transmembrane domains anchor authentic atTic110 to the membrane.

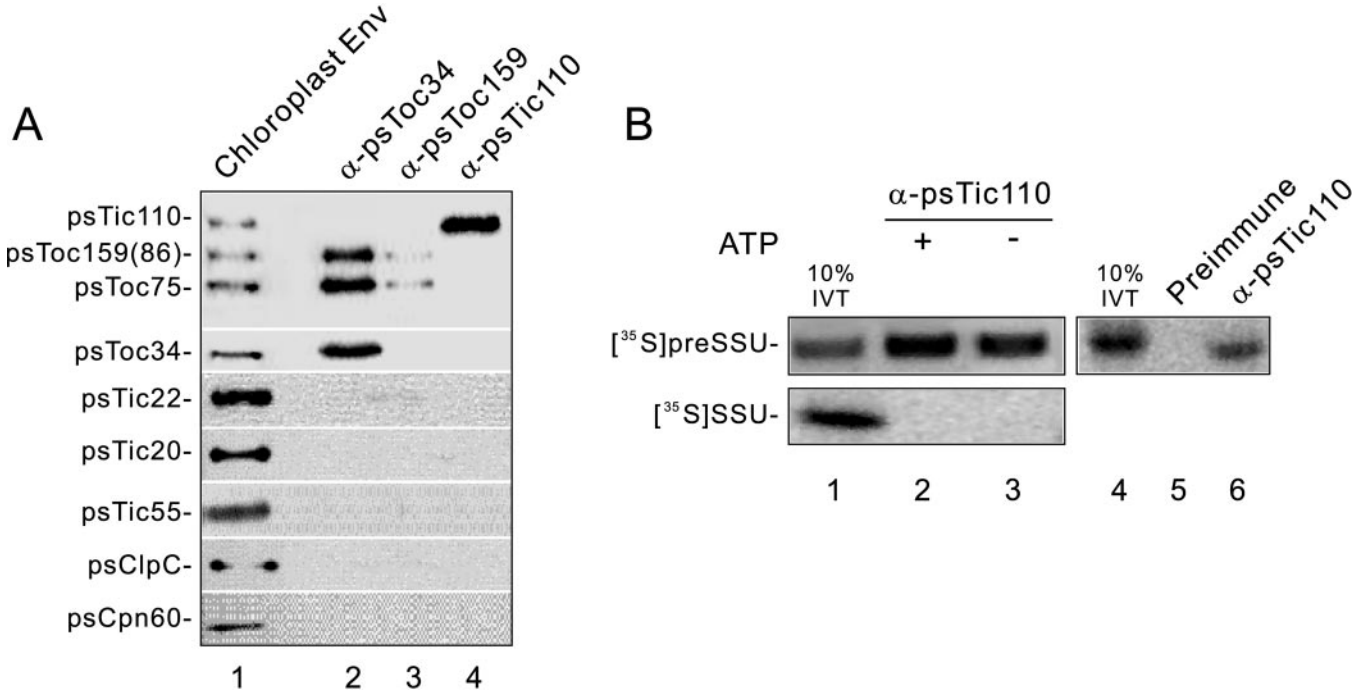

FIG. 5. **Direct binding of preprotein to chloroplast-derived psTic110.** *A*, a total chloroplast envelope membrane fraction (100 μg of protein) was dissolved in TES buffer containing 1% Triton X-100 and subjected to sequential immunoaffinity chromatography on anti-psToc34-Sepharose (*α-psToc34*), anti-psToc159-Sepharose (*α-psToc159*), and anti-psTic110-Sepharose (*α-psTic110*). The eluates from each chromatography step were analyzed by SDS-PAGE and immunoblotting with the antisera specific for the proteins indicated at the *left* of the figure. *B*, *in vitro* translated (*IVT*) [^{35}S]pre-SSU or [^{35}S]SSU was incubated in the presence or absence of ATP with psTic110 bound to anti-psTic110-Sepharose (*lane 4*, *A*) or preimmune IgG-Sepharose. Bound translation products were analyzed by SDS-PAGE and phosphorimaging analysis. The positions of [^{35}S]pre-SSU and [^{35}S]SSU are shown to the *left* of the figure. *Lanes 1* and *4* contain 10% of the *in vitro* translation products added to the binding reactions.

Purified atTic110 Binds to Chloroplast Preproteins—Upon establishing that atTic110$_{93–966}$ exists as a soluble stromal domain, we wished to examine the hypothesis that it coordinates the late events in preprotein translocation in the stroma. A psTic110-chaperone complex is proposed to bind preproteins as they emerge from the protein-conducting channel of the Tic complex (12). However, it has not been determined whether Tic110 forms the initial *trans*-docking site at the translocon by binding directly to preproteins or participates indirectly by bringing chaperones to the site of translocation. To address this question, we first investigated the ability of native psTic110 to interact with preproteins using covalent cross-linking and preprotein binding approaches. We have previously used a label transfer cross-linking approach to map the interactions of preproteins with the import machinery during the course of protein import (27). However, these experiments could not resolve proteins in the higher molecular weight range, including Tic110. Therefore, we analyzed cross-linked products on a 7.5–15% gradient gel to resolve psTic110 from the Toc components.

Isolated pea chloroplasts were incubated with pFd-protA-[^{125}I]APDP, a chimeric chloroplast preprotein consisting of preferredoxin fused to staphylococcal protein A, that had been modified with a label-transfer cross-linking reagent ([^{125}I]APDP) (27). pFd-protA-[^{125}I]APDP was bound in the absence or presence of ATP and GTP, and cross-linking to nearby proteins was induced by UV light. Reduction of the cross-linking reaction results in the transfer of the ^{125}I label to the cross-linked target and release of the bound preprotein. Previous studies have shown that the pFd-protA-[^{125}I]APDP fusion protein binds exclusively to the Toc complex in the absence of energy (27). The results in Fig. 4*A* are consistent with the previous observations. Two Toc components, Toc159 and Toc75, are the major cross-linked products (Fig. 4*A*, *lane 1*). In the presence of energy, the preprotein forms an import intermediate that spans both the Toc and Tic translocons. Under these conditions, Toc75 and two Tic components, Tic22 and Tic20, are cross-linked to the preprotein as previously observed (Fig. 4*A*, *lane 2*). In addition, a 110-kDa cross-linked polypeptide was apparent (Fig. 4*A*, *lane 2*, *asterisk*). Immunoprecipitation of the detergent-solubilized cross-linking reaction with anti-psTic110 serum demonstrated that the cross-linked product was psTic110 (Fig. 4*B*, *lane 1*). These data suggest that Tic110 and preprotein are in close proximity during translocation at the Tic translocon.

To further investigate the possibility of a direct interaction between Tic110 and preprotein, we purified psTic110 from the envelope of pea chloroplasts and asked whether it could bind preproteins. A chloroplast envelope fraction enriched in inner membrane vesicles was dissolved with detergent under native conditions. The soluble extract was incubated with ATP to disrupt interactions between Tic110 and its two associated chaperones, Hsp93 and Cpn60 (12, 20). The fraction then was subjected to sequential immunadsorbtions with two Toc antisera, anti-psToc34 and anti-psToc159, to deplete any Toc-Tic supercomplexes that could contaminate the psTic110 fraction. Finally, psTic110 was adsorbed from the depleted membrane sample using anti-psTic110 bound to Sepharose. Analysis of this fraction demonstrated that immunoadsorbed psTic110 was free of associated chaperones, Toc components, and other known Tic components (Fig. 5*A*). The immunoadsorbed psTic110 was incubated with the precursor ([^{35}S]pre-SSU) or mature ([^{35}S]SSU) forms of the small subunit of rubisco to test its ability to specifically bind a chloroplast preprotein. As shown in Fig. 5*B*, [^{35}S]pre-SSU was specifically coimmunoprecipitated with psTic110, whereas [^{35}S]SSU exhibited no detectable binding. The association was not sensitive to ATP, providing additional evidence that the observed binding was not due to the presence of residual chaperones (Fig. 5*B*, compare *lanes 2* and *3*). Furthermore, the antibodies from the preimmune serum did not bind [^{35}S]pre-SSU (Fig. 5*B*, *lane 5*). In conjunc-

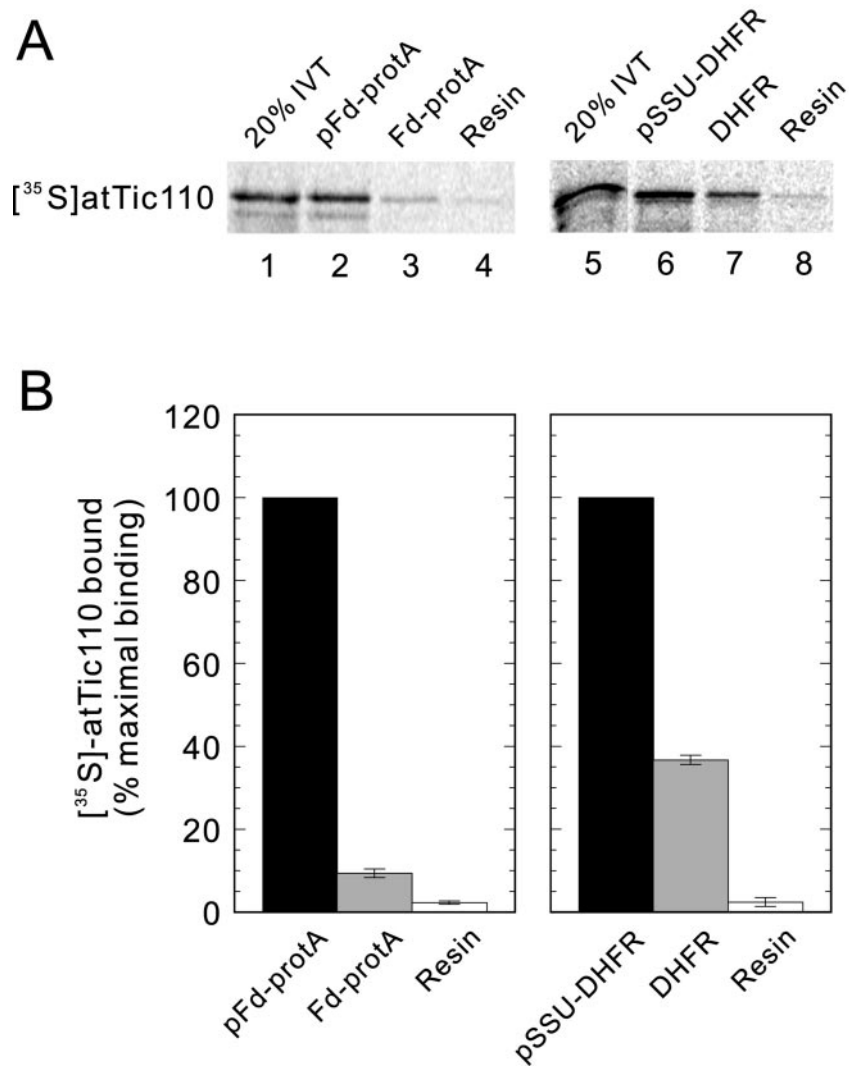

FIG. 6. **Binding of atTic110 to chloroplast preproteins.** *A*, recombinant pFd-protA, Fd-protA, pSSU-DHFR, or DHFR were immobilized on nickel-NTA resin and incubated with *in vitro* translated [^{35}S]atTic110. Bound [^{35}S]atTic110 was eluted and analyzed directly by SDS-PAGE and phosphorimaging analysis. *Lanes 1* and *5* contain 20% of the *in vitro* translated [^{35}S]atTic110 added to each binding reaction. *B*, quantitative analysis of data from triplicate experiments including those shown in *A* with *bars* indicating the standard error.

tion with the covalent cross-linking studies, our data indicate that native Tic110 from chloroplasts directly binds to preproteins via their intrinsic transit peptides.

Direct Interaction between atTic110 and Preproteins—The observation that Tic110 from pea chloroplasts associates with a chloroplast preprotein led us to investigate the requirements and specificity of binding using the recombinant atTic110 constructs. To this end, we developed a preprotein binding assay using immobilized preprotein fusions and *in vitro* translated [^{35}S]atTic110. Hexahistidine-tagged preprotein fusions, pFd-protA and pSSU-DHFR, and their corresponding mature forms lacking transit peptides, Fd-protA and DHFR, were immobilized on a nickel-NTA resin and incubated with [^{35}S]atTic110. As shown in Fig. 6*A*, [^{35}S]atTic110 bound to pFd-protA at greater than 10-fold higher levels compared with Fd-protA. The level of binding to Fd-protA was similar to the background binding observed with nickel-NTA resin alone (Fig. 6*B*). [^{35}S]atTic110 binding to pSSU-DHFR was 3-fold higher than that observed with DHFR (Fig. 6*A*). DHFR consistently exhibited higher nonspecific binding to all constructs tested (data not shown). The efficiency of binding to both pFd-protA and pSSU-DHFR was 15–20% of added [^{35}S]atTic110 (Fig. 6*A*). Negligible binding was observed to the nickel-NTA resin alone (Fig. 6*A*). These data confirm the ability of atTic110 to bind preproteins and demonstrate that binding is conferred by the preprotein transit peptide.

The Preprotein-binding Site of atTic110 Is Localized to the Soluble Carboxyl-terminal Region—As a next step in our analysis, we wished to examine the binding specificity and define the transit peptide binding region of atTic110. For this purpose, we tested the ability of the recombinant atTic110 deletion constructs (Fig. 1) to compete with [^{35}S]atTic110 for binding to pFd-protA. For these assays, pFd-protA lacking a hexahistidine tag was immobilized on IgG-Sepharose and incubated with [^{35}S]atTic110 in the absence or presence of the competitor. Both atTic110$_{93–966}$ and atTic110$_{185–966}$ efficiently inhibit the binding of [^{35}S]atTic110 to pFd-protA (Fig. 7*A*). The inhibition by both proteins is dose-dependent with maximum inhibition observed between 200 and 500 nM competitor (Fig. 7*B*). In contrast, atTic110$_{370–966}$ does not efficiently inhibit the binding of [^{35}S]atTic110 to pFd-protA (Fig. 7), suggesting that this deletion construct lacks the transit peptide-binding site. An unrelated protein, CRABP, has no effect on [^{35}S]atTic110 binding at the highest concentration tested (Fig. 7). These data demonstrate that the interaction between [^{35}S]atTic110 and the preprotein is specific and suggest that at least part of the transit peptide-binding domain is located within the amino-terminal region of atTic110.

To confirm direct binding of atTic110$_{185–966}$ to preproteins, we tested its ability to bind immobilized pFd-protA and pSSU-DHFR. Fig. 8 shows that *in vitro* translated [^{35}S]atTic110$_{185–966}$ binds pFd-protA and pSSU-DHFR (Fig. 8) with a selectivity nearly identical to that observed with full-length atTic110. It should be noted that the binding efficiency

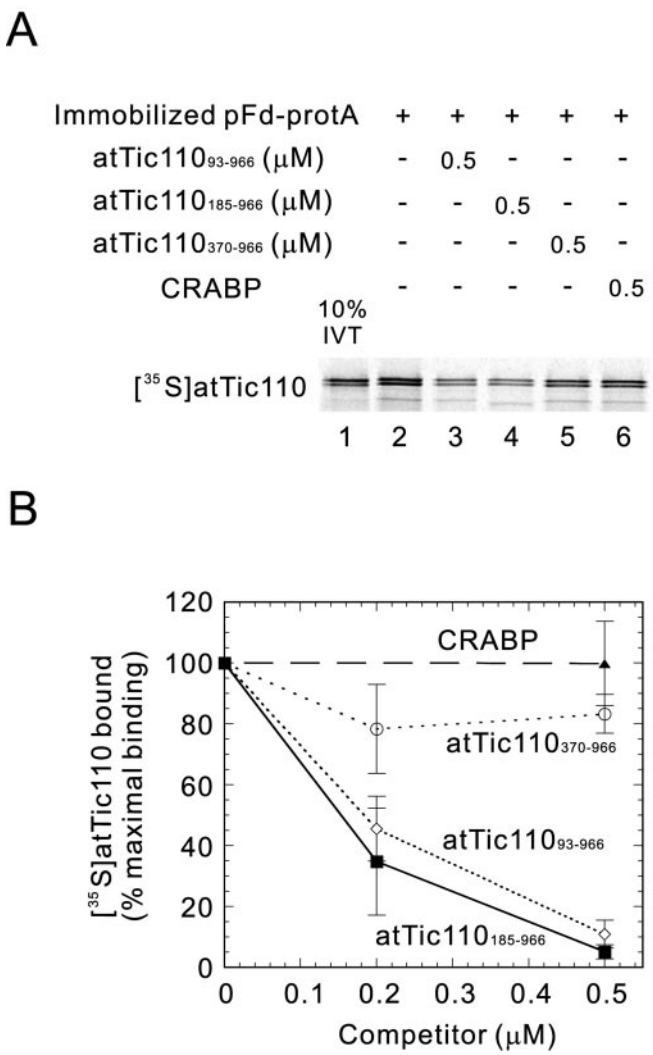

FIG. 7. **Localization of the preprotein binding site of atTic110 to the soluble carboxyl-terminal region.** *A*, *in vitro* translated (*IVT*) [^{35}S]atTic110 was incubated with pFd-protA immobilized on IgG-Sepharose in the absence or presence of 0.5 μM atTic110$_{93-966}$, atTic110$_{185-966}$, atTic110$_{370-966}$, or CRABP. Bound [^{35}S]atTic110 was eluted and analyzed directly by SDS-PAGE and phosphorimaging analysis. *Lane 1* contains 10% of the *in vitro* translated [^{35}S]atTic110 added to each binding reaction. *B*, quantitative analysis of [^{35}S]atTic110 binding to pFd-protA in the presence of increasing concentrations of the competitors used in *A*. Each point represents the mean of triplicate experiments with *bars* indicating the standard error.

of [^{35}S]atTic110$_{185-966}$ to pFd-protA and pSSU-DHFR is ~20% of that observed with full-length atTic110 (Fig. 6), suggesting that [^{35}S]atTic110$_{185-966}$ contains a minimal transit peptide-binding site. [^{35}S]atTic110$_{370-966}$ does not bind to pFd-protA or pSSU-DHFR (Fig. 8*A*), consistent with its inability to compete with the binding of full-length atTic110 (Fig. 7). On the basis of the results in Figs. 7 and 8, we conclude that residues 185–370 form at least part of a binding site for preprotein transit peptides on atTic110.

The role of residues 185–370 in transit peptide binding was explored further by testing the ability of a carboxyl-terminal deletion construct of atTic110, atTic110$_{1-602}$ (Fig. 1), to bind preproteins. As shown in Fig. 9 (*A* and *B*), [^{35}S]atTic110$_{1-602}$ binds to pFd-protA and pSSU-DHFR. This construct exhibited similar binding affinities and specificities as we observed with [^{35}S]atTic110 (Fig. 6*A*). The binding of [^{35}S]atTic110$_{1-602}$ to pFd-protA was inhibited effectively in a dose-dependent manner by recombinant atTic110$_{185-966}$ (Fig. 9, *C* and *D*) at concentrations comparable with those that competed binding of [^{35}S]atTic110 (Fig. 7). atTic110$_{370-966}$ was not an effective competitor at the concentrations tested (Fig. 9*D*). Our results indicate that the region between Met^{185} and Met^{370} encompasses a preprotein-binding domain on atTic110. In total, these data indicate that the carboxyl-terminal, stromal domain of Tic110 forms a *trans*-binding site for the transit peptide of preproteins during translocation through the Tic translocon at the inner envelope membrane.

DISCUSSION

In this paper, we have focused on the role of Tic110 as a component of the protein translocon at the inner envelope of chloroplasts. Our goal was to examine the hypotheses that Tic110 functions primarily as a docking site for stromal import factors (12, 20), an inner membrane-anchored protein of the intermembrane space that mediates Toc and Tic translocon interactions (13, 19), or a β-barrel membrane channel for the Tic translocon (23). Our analyses demonstrate that the carboxyl-terminal 97.5 kDa of atTic110 folds into a soluble domain when expressed both in *E. coli* (Fig. 2) and in *Arabidopsis* (Fig. 3), supporting the conclusion that this region forms a hydrophilic stromal domain. Structural studies confirm that the region consists predominantly of α-helical structure (Fig. 2). Furthermore, we provide both *in organello* and *in vitro* evidence that Tic110 binds directly to preproteins (Figs. 4–6) and demonstrate that a segment of the carboxyl-terminal domain mediates this association (Fig. 8). In total, our results support the hypothesis that the bulk of Tic110 forms a stromal docking site for factors involved in the late stages of protein import (12, 20) and extend the activities of the protein to include transit peptide binding at the stromal face of the Tic translocon.

psTic110 originally was isolated as a component of an import intermediate associated complex containing a bound preprotein (3, 12, 13) and psTic110 antibodies coimmunoprecipitated preproteins bound to the Tic complex (12, 22). Furthermore, preproteins appear to bind specifically to inverted inner envelope vesicles (23), consistent with our proposal that the transit peptide-binding site of Tic110 lies at the inner face of the inner membrane. However, these previous studies did not distinguish between the direct binding of preproteins to Tic110 and an indirect interaction mediated by the binding of preproteins to Tic110-associated molecular chaperones or other import components. Our data demonstrate that atTic110 possesses a transit peptide-specific binding site for preproteins.

Although the exact conformation of Tic110 remains to be established, the localization of the transit peptide-binding site between Met^{185} and Met^{370} on atTic110 (Figs. 7–9) suggests that the site lies adjacent to the exit site of the Tic translocon. Interestingly, secondary structure prediction suggests that the transit peptide-binding region is rich in α-helices, containing at least two amphipathic helices with acidic faces between residues 180–200 and 280–300. Although more detailed structure/function analysis is required, it is intriguing to speculate that these regions could interact with transit peptides, all of which tend to have overall basic characteristics.

The transit peptide binding data and previous reports establishing the direct association of psTic110 with stromal chaperones led us to propose a model in which Tic110 coordinates the coupling of translocation and chaperone binding at the stromal face of the chloroplast inner membrane. On the basis of this observation, we hypothesize that Tic110 provides a transit peptide-docking site for preproteins as they emerge from the protein-conducting channel of the Tic translocon. This docking could prevent reverse translocation of the imported preprotein, thereby conferring unidirectional transport into the stroma. The docking of the chloroplast Hsp93 homologue (chloroplast ClpC) at Tic110 (22, 30) would concentrate this chaperone at

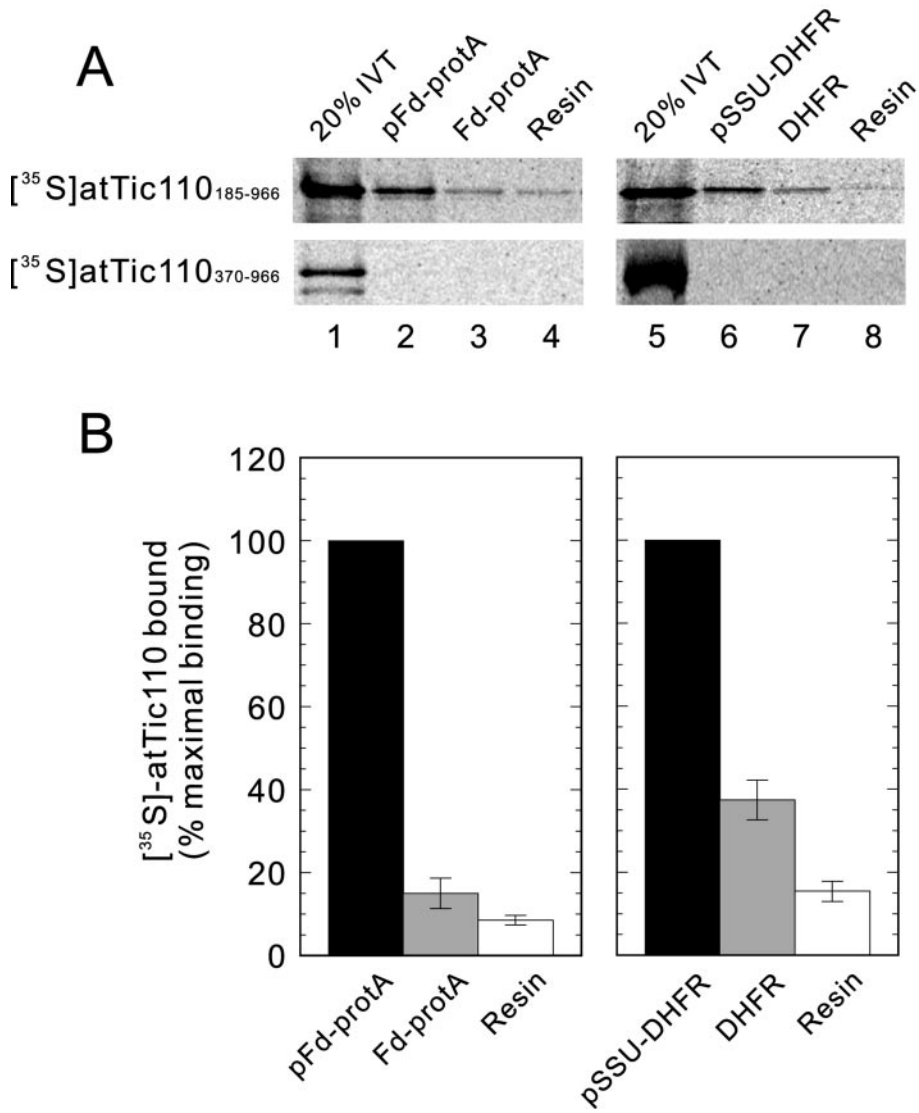

FIG. 8. **Direct binding of atTic-110$_{185–966}$ and atTic110$_{370–966}$ to chloroplast preproteins.** *A*, *in vitro* translated (*IVT*) [^{35}S]atTic110$_{185–966}$ or [^{35}S]atTic110$_{370–966}$ was incubated with immobilized pFd-protA, Fd-protA, pSSU-DHFR, or DHFR as described under "Experimental Procedures." Bound [^{35}S]atTic110$_{185–966}$ or [^{35}S]atTic110$_{370–966}$ was eluted and analyzed directly by SDS-PAGE and phosphorimaging analysis. *Lanes 1* and *5* contain 20% of the *in vitro* translated [^{35}S]atTic110$_{185–966}$ or [^{35}S]atTic110$_{370–966}$ added to each binding reaction. *B*, quantitative analysis of data from [^{35}S]atTic110$_{185–966}$ binding (*upper panel* of *A*) with *bars* indicating the standard error of triplicate experiments.

the exit site of the translocon and facilitate its binding to the trapped preprotein. Binding of Hsp93 presumably prevents misfolding/aggregation and provides the driving force for complete translocation into the stroma (22). The association of the chloroplast GroEL homologue, Cpn60, with Tic110 (12) would facilitate folding of the newly imported protein before it diffuses from the site of translocation. In this regard, Tic110 would function in a manner analogous to Tim44 of the mitochondrial Tim17/23 translocon and Sec63 of the translocon of the endoplasmic reticulum, both of which coordinate the binding of chaperones to translocating polypeptides (31).

Cleavage of the transit peptide is known to occur very early in the translocation reaction (32). Processing by the stromal processing peptidase would result in release of the preprotein from Tic110, allowing translocation to proceed. It is interesting to speculate that stromal processing peptidase might also transiently interact with the Tic110 to catalyze transit peptide hydrolysis and dissociation. As such, Tic110 would serve as a molecular scaffold that coordinates the translocation, processing, and folding of preproteins at the Tic translocon. The assembly of the stromal factors mediating these events would generate a protected environment for the maturation of newly imported preproteins similar to that envisioned in the lumen of the endoplasmic reticulum (31). Future studies will reveal the degree to which Tic110 plays an active or passive role in the coordination of these events.

The expression and CD data presented here are in contrast with the proposal that Tic110 forms a protein-conducting channel with stable β-barrel structure. The results from the previous study (23) were based on the use of a reconstituted system consisting of a urea-denatured carboxyl-terminal fragment of psTic110 that was incorporated into liposomes. This fragment corresponded to residues 178–958 of psTic110, a construct very similar to the atTic110$_{185–966}$ deletion mutant used in this study. The analysis of the secondary structure content of the detergent-stabilized protein prior to insertion into liposomes indicated a lack of α-helices consistent with high β-strand content (23). Our results using native atTic110$_{370–966}$, atTic110$_{185–966}$, and atTic110$_{93–966}$ indicate a high α-helical content consistent with secondary structure predictions. It is unlikely that the difference in the results can be attributed to differences in the primary structures of the *Arabidopsis* and pea proteins, because the carboxyl-terminal regions exhibit 70% sequence identity throughout their primary structures (data not shown).

Previous targeting and topology studies also support the conclusion that Tic110 consists largely of a hydrophilic stromal domain with short transmembrane anchors at its extreme amino terminus. Topology mapping assays in intact chloroplasts (12, 20) and isolated inner envelope membrane vesicles (20, 23) have shown that the protease sensitivity of the carboxyl-terminal region of psTic110 is identical to authentic stromal

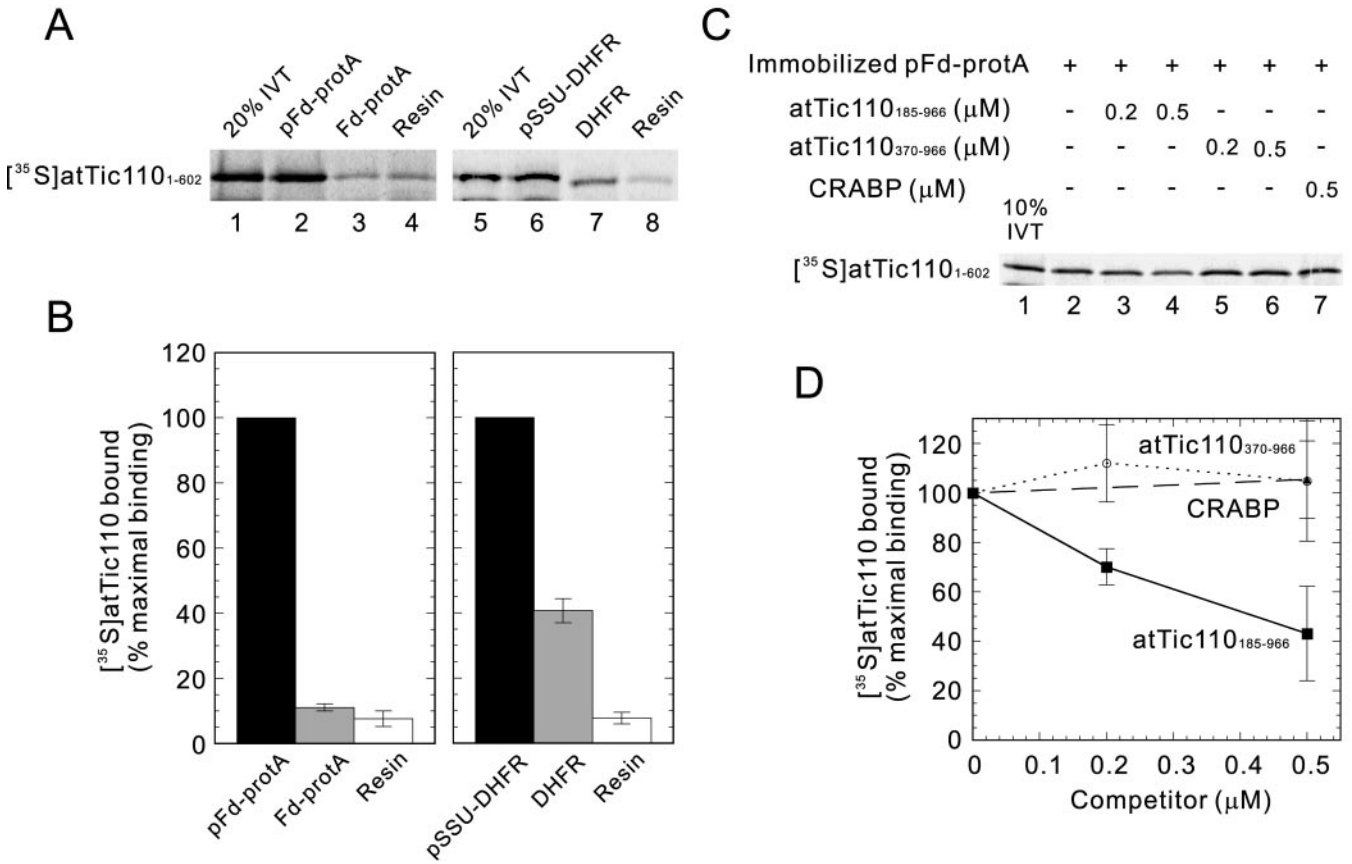

FIG. 9. **Direct binding of atTic110$_{1-602}$ to chloroplast preproteins.** *A*, *in vitro* translated (*IVT*) [^{35}S]atTic110$_{1-602}$ was incubated with immobilized pFd-protA, Fd-protA, pSSU-DHFR, or DHFR as described in the legend to Fig. 6. Bound [^{35}S]atTic110$_{1-602}$ was eluted and analyzed directly by SDS-PAGE and phosphorimaging analysis. *Lane 1* contains 20% of the *in vitro* translated [^{35}S]atTic110$_{1-602}$ added to each binding reaction. *B*, quantitative analysis of data from triplicate experiments including those shown in *A* with *bars* indicating the standard error. *C*, *in vitro* translated [^{35}S]atTic110$_{1-602}$ was incubated with IgG-Sepharose-immobilized pFd-protA in the absence or presence of increasing concentrations of atTic110$_{185-966}$, atTic110$_{370-966}$, or CRABP. Bound [^{35}S]atTic110$_{1-602}$ was eluted and analyzed directly by SDS-PAGE and phosphorimaging analysis. *Lane 1* contains 10% of the *in vitro* translated [^{35}S]atTic110 added to each binding reaction. *D*, quantitative analysis of data from triplicate experiments including those shown in *C* with *bars* indicating the standard error.

proteins that associate peripherally with the inner face of the inner membrane (20) and is distinct from proteins of the outer envelope and intermembrane space (12, 20, 23). Our results also support these observations (Fig. 3*D*). These data indicate that the carboxyl terminus is not exposed at the outer surface of the inner membrane as would be expected if the domain formed multiple membrane spans. The topology studies also discount another proposal that this domain extends into the intermembrane space and interacts with the Toc machinery (13). Targeting studies using fusion proteins containing the amino-terminal region of psTic110 demonstrated that this region was necessary and sufficient for targeting and anchoring authentic psTic110 to the inner membrane (19), supporting this region as the Tic110 membrane anchor.

A channel with characteristics similar to that measured using the reconstituted psTic110 fragment is not observed in chloroplasts or isolated inner envelope membranes (23), raising questions about the physiological relevance of the reconstitution data. Furthermore, reconstitution of native psTic110 into proteoliposomes does not yield a channel similar to that observed with the denatured fragment (23). A protein import related anion channel (PIRAC) has previously been identified in intact chloroplasts (33, 34) with conductance characteristics distinct from the reconstituted psTic110 fragment. PIRAC activity was efficiently inhibited by authentic preferredoxin but not import incompetent deletion mutants (35), indicating that PIRAC was specifically linked to protein import. Similar selective activity was not demonstrated for the reconstituted psTic110 fragment (23). Interestingly, antibodies to psTic110 inhibited the PIRAC channel, consistent with the observation that Tic110 is closely associated with the inner membrane translocation channel. In fact, we do not exclude the possibility that the amino-terminal transmembrane region of Tic110 participates directly in translocation by forming a part of the Tic protein-conducting channel. Furthermore, we cannot rule out the possibility entirely that the carboxyl-terminal domain might undergo a reversible conformational change in response to preprotein translocation that results in the insertion of this region into the inner membrane in a β-barrel structure. Such dramatic conformational shifts have been observed for a specialized group of bacterial toxins (36). However, there is no evidence to support such a switch in Tic110 conformation, and the structural and topology studies make it highly unlikely that the carboxyl-terminal region forms a β-barrel.

Tic110 associates dynamically with Tic20 (11), an integral inner membrane Tic component, with similarity to the Tim17/23 channel components of a mitochondrial inner membrane protein translocon (11). We have provided genetic and biochemical evidence that Tic20 participates in inner membrane translocation (14). Therefore, it is possible that Tic110 and Tic20 assemble with other Tic proteins in response to translocation across the outer membrane to form the Tic channel and provide a *trans*-binding site to initiate preprotein translocation across the inner membrane.

Acknowledgments—We thank Matthew D. Smith and Caleb M. Rounds (University of Massachusetts, Amherst, MA) for generous gifts of pSSU-DHFR and DHFR proteins and Dr. Lila Gierasch (University of Massachusetts, Amherst, MA) for technical assistance and providing purified recombinant CRABP.

REFERENCES

1. Keegstra, K., and Cline, K. (1999) *Plant Cell* **11,** 557–570
2. Bauer, J., Hiltbrunner, A., and Kessler, F. (2001) *Cell. Mol. Life Sci.* **58,** 420–433
3. Kessler, F., Blobel, G., Patel, H. A., and Schnell, D. J. (1994) *Science* **266,** 1035–1039
4. Bauer, J., Chen, K., Hiltbunner, A., Wehrli, E., Eugster, M., Schnell, D., and Kessler, F. (2000) *Nature* **403,** 203–207
5. Hiltbrunner, A., Bauer, J., Vidi, P. A., Infanger, S., Weibel, P., Hohwy, M., and Kessler, F. (2001) *J. Cell Biol.* **154,** 309–316
6. Bauer, J., Hiltbrunner, A., Weibel, P., Vidi, P. A., Alvarez-Huerta, M., Smith, M. D., Schnell, D. J., and Kessler, F. (2002) *J. Cell Biol.* **159,** 845–854
7. Smith, M. D., Hiltbrunner, A., Kessler, F., and Schnell, D. J. (2002) *J. Cell Biol.* **159,** 833–843
8. Schnell, D. J., Kessler, F., and Blobel, G. (1994) *Science* **266,** 1007–1012
9. Ma, Y., Kouranov, A., LaSala, S., and Schnell, D. J. (1996) *J. Cell Biol.* **134,** 315–327
10. Hinnah, S. C., Hill, K., Wagner, R., Schlicher, T., and Soll, J. (1997) *EMBO J.* **16,** 7351–7360
11. Kouranov, A., Chen, X., Fuks, B., and Schnell, D. J. (1998) *J. Cell Biol.* **143,** 991–1002
12. Kessler, F., and Blobel, G. (1996) *Proc. Natl. Acad. Sci. U. S. A.* **93,** 7684–7689
13. Lubeck, J., Soll, J., Akita, M., Nielsen, E., and Keegstra, K. (1996) *EMBO J.* **15,** 4230–4238
14. Chen, X., Smith, M. D., Fitzpatrick, L., and Schnell, D. J. (2002) *Plant Cell* **14,** 641–654
15. Kouranov, A., Wang, H., and Schnell, D. J. (1999) *J. Biol. Chem.* **274,** 25181–25186
16. Stahl, T., Glockmann, C., Soll, J., and Heins, L. (1999) *J. Biol. Chem.* **274,** 37467–37472
17. Caliebe, A., Grimm, R., Kaiser, G., Lubeck, J., Soll, J., and Heins, L. (1997) *EMBO J.* **16,** 7342–7350
18. Kuchler, M., Decker, S., Hormann, F., Soll, J., and Heins, L. (2002) *EMBO J.* **21,** 6136–6145
19. Lubeck, J., Heins, L., and Soll, J. (1997) *J. Cell Biol.* **137,** 1279–1286
20. Jackson, D. T., Froehlich, J. E., and Keegstra, K. (1998) *J. Biol. Chem.* **273,** 16583–16588
21. Schneider, H. C., Berthold, J., Bauer, M. F., Dietmeier, K., Guiard, B., Brunner, M., and Neupert, W. (1994) *Nature* **371,** 768–774
22. Nielsen, E., Akita, M., Davila-Aponte, J., and Keegstra, K. (1997) *EMBO J.* **16,** 935–946
23. Heins, L., Mehrle, A., Hemmler, R., Wagner, R., Kuchler, M., Hormann, F., Sveshnikov, D., and Soll, J. (2002) *EMBO J.* **21,** 2616–2625
24. Pelton, J. T., and McLean, L. R. (2000) *Anal. Biochem.* **277,** 167–176
25. Jones, D. T. (1999) *J. Mol. Biol.* **292,** 195–202
26. Smith, M. D., Fitzpatrick, L. M., Keegstra, K., and Schnell D. J. (2002) in *Current Protocols in Cell Biology* (Bonifacino, J. S., Harford, J. B., Lippincott-Schwartz, J., and Yamada, K. M., eds) pp. 11.16.11–11.16.21, John Wiley & Sons, Inc., New York
27. Kouranov, A., and Schnell, D. J. (1997) *J. Cell Biol.* **139,** 1677–1685
28. Keegstra, K., and Yousif, A. E. (1986) *Methods Enzymol.* **118,** 316–325
29. Anderson, D. J., and Blobel, G. (1983) *Methods Enzymol.* **96,** 111–120
30. Akita, M., Nielsen, E., and Keegstra, K. (1997) *J. Cell Biol.* **136,** 983–994
31. Schnell, D. J., and Hebert, D. N. (2003) *Cell* **112,** 491–505
32. Schnell, D. J., and Blobel, G. (1993) *J. Cell Biol.* **120,** 103–115
33. van den Wijngaard, P. W. J., and Vredenberg, W. J. (1997) *J. Biol. Chem.* **272,** 29430–29433
34. van den Wijngaard, P. W., and Vredenberg, W. J. (1999) *J. Biol. Chem.* **274,** 25201–25204
35. van den Wijngaard, P. W., Demmers, J. A., Thompson, S. J., Wienk, H. L., de Kruijff, B., and Vredenberg, W. J. (2000) *Eur. J. Biochem.* **267,** 3812–3817
36. Heuck, A. P., Tweten, R. K., and Johnson, A. E. (2001) *Biochemistry* **40,** 9065–9073